SENSITIVITY ANALYSIS OF ACCELEROMETERS FOLLOWING THERMAL CYCLING

Emily Bond [(1)], Charly Knight [(2)], Thomas Fielding [(3)]

[(1)] RAL Space, Science and Technology Facilities Council, Rutherford Appleton Laboratory, Harwell Campus, Didcot, OX11 0QX, United Kingdom, (ebond04@qub.ac.uk)
[(2)] RAL Space, Science and Technology Facilities Council, Rutherford Appleton Laboratory, Harwell Campus, Didcot, OX11 0QX, United Kingdom, (charly.knight@stfc.ac.uk)
[(3)] RAL Space, Science and Technology Facilities Council, Rutherford Appleton Laboratory, Harwell Campus, Didcot, OX11 0QX, United Kingdom, (thomas.fielding@stfc.ac.uk)

KEYWORDS

Accelerometers, Sensitivity Shift, Thermal Cycling

ABSTRACT

Accelerometers see applications in a range of industries, frequently seeing installation on spacecraft ahead of thermal testing before dynamic testing. However, the current studies and specifications see minimal investigation of the effect of thermal cycling on shock and vibration accelerometers. This paper details a multi-stage and phase testing profile. The testing profile and methodology used throughout this work enabled a comparison of two different accelerometer types (vibration and shock) as well as an investigation of the sensitivity-temperature dependency of each model of accelerometer.

Sensitivity analysis following the testing shows all accelerometers survived and continued to function correctly after being held at steady state extreme high and low temperatures. However, after the extended cycling, some accelerometers exceeded the allowable ±5% deviation limits on sensitivity.

1. INTRODUCTION

Accelerometers allow for the measurement of static or dynamic acceleration on moving or vibrating bodies [1]. Accelerometers are typically classified by the number of axes: monoaxial, biaxial, and triaxial, and via the sensor technology under which it operates, namely piezoelectric, piezoresistive, and capacitive [2].

Piezoelectric accelerometers typically see use in vibration testing, shock testing, and hydraulic perturbations due to their ability to measure high-frequency signals [3]. Piezoresistive accelerometers, however, are not suitable for vibration testing due to their low sensitivity; instead, they see applications in crash or weapons testing due to high bandwidth allowing high-frequency measurements in a short duration [4]. Capacitive accelerometers have limited bandwidth (a few hundred hertz) due to physical geometry, favouring a lower range of acceleration, making them suitable for airbags and mobile devices [4]. While each type of accelerometer has its advantages and disadvantages, piezoelectric accelerometers have continuously seen increased use due to their reduced geometry, broad bandwidth, and inbuilt charge converter [4], seeing further use in the vibration test phase of assembly integration and verification (AIV) of a spacecraft.

When selecting an accelerometer, many properties must be considered, including but not limited to sensitivity, operating temperature, number of axes, sensor technology, and required application. Sensitivity refers to the ratio of change in accelerometer output to the change of applied acceleration, usually at a reference frequency [5]. Often accelerometer datasheets will have an acceptable operating temperature and a stated sensitivity variation with temperature. The dependency between sensitivity and temperature occurs because circuit board temperature coefficients along with temperature-induced mechanical stresses alter the accelerometer's mechanical components [5]. Due to the influence of temperature on accelerometer sensitivity, it is important that calibrations are checked frequently to ensure that the sensitivity has not deviated past the standard tolerance of ±5% or ±10% of the stated nominal sensitivity [6].

Current studies regarding exposure of accelerometers to a thermal environment have primarily seen testing of MEMS (Micro Optical Electro Mechanical Systems) accelerometers in simultaneous vibration and high temperature testing [7], simultaneous tilting and high-temperature & bias [7], and characterisation under standardised tests [8]. The study by Bâzu *et al.* [7] focused on quantitative accelerated life testing with vibration as the chosen mechanical stress, based on MEMS normal usage, as well as a high temperature due to the unlikelihood of thermal cycling during operational life. Following testing, firstly, at 85 ˚C at 1500Hz followed by 145 ˚C at 1500Hz, there was a minimal performance degradation after 100 hours of testing.

Although current specifications showed the sensitivity deviation at a specific temperature, at the time of this study, no specifications or current studies could be found that detailed the impact of a varied temperature profile over an extended period on the sensitivity of accelerometers, especially piezoelectric which left scope for investigation.

Based on current studies and available resources, this work aimed to investigate the sensitivity shift of four piezoelectric vibration accelerometers and four piezoelectric shock accelerometers following thermal cycling. With the outlined aim, this work included cycling of accelerometers at a constant high temperature, followed by a constant low temperature, and then finally steady cycling. A vibration calibration rig was used to determine accelerometer sensitivities at a reference level and allow for monitoring of any deviation above or below the ±5% deviation limits.

2. METHODS

2.1. Accelerometer Properties

This study focused on four shock accelerometers (350M88A, ICP® Shock Accelerometer, PCB Piezotronics) and four vibration accelerometers (356A43, Triaxial ICP® Accelerometer, PCB Piezotronics), the key properties of which are detailed in Table 1 and Table 2, respectively.

Table 1: 350M88A Accelerometer Properties

Item	Parameter
Sensitivity (± 30%)	0.5 mV/g
Frequency Range (± 1 dB)	0.4 to 10,000 Hz
Temperature Range (Operating)	-23 to +66 ˚C
Temperature Range (Storage)	-40 to +93 ˚C
Sensing Element	Ceramic
Sensing Geometry	Shear
Housing Material	Titanium
Size (Hex x Height)	9.5 mm x 24.1 mm

Table 2: 356A43 Accelerometer Properties

Item	Parameter
Sensitivity (± 10%)	10 mV/g
Frequency Range (± 5%)	0.7 to 7000 Hz
Temperature Range (Operating)	-54 to +121 ˚C
Sensing Element	Ceramic
Sensing Geometry	Shear
Housing Material	Titanium
Size	10.2 mm x 19.1 mm x 10.2 mm

Each vibration cable (034M22, Low outgas cable assembly, 4-Pin, to 3 BNC, 20ft. PCB Piezotronics) was paired with a vibration accelerometer and subsequently labelled with the corresponding serial number. Removal of vibration cables was primarily due to their low outgassing property, making them potentially unsuitable for the test temperatures. It also served to reduce the number of variables present in testing. Shock accelerometer cables were integrated so, therefore, did not require labelling.

2.2. Calibration Check

Before testing, as well as prior to commencing the next test stage or phase, each accelerometer was calibrated using a vibration calibration rig (9155D-830, K393B30, Air Bearing Calibration Shaker, The Modal Shop), using a reference frequency of 160Hz for vibration accelerometers and 100Hz for shock accelerometers. Tab. 3 shows the testing stages and phases and their corresponding calibration check point(s). All calibration checks and starting of the next stage/ phase occurred within 48 hours of ending the previous test stage/ phase, except for stage 1: phase 3, which aligned with an extended break period. As a result, a calibration check point was conducted before the break and before commencing stage 2 testing. This was to check whether the time had an impact on the results.

Table 3: Testing stages and phases with corresponding calibration check point

Testing Stage/ Phase	Calibration Check Point
Before testing	0
Stage 1: Phase 1	1
Stage 1: Phase 2	2
Stage 1: Phase 3	3 and 4
Stage 2: Phase 1	5
Stage 2: Phase 2	6
Stage 2: Phase 3	7
Stage 3	8

The system was verified before calibration to ensure that the output sensitivities were as accurate as possible, using a reference accelerometer. In addition, calibration checks for all accelerometers (all axes for vibration accelerometers) were repeated 5 times to improve the accuracy of measurement. The frequencies and amplitude at which the accelerometers were tested are detailed in Table 4.

Table 4: Calibration test frequencies and amplitudes

Frequency (Hz)	Amplitude (g)
5.00	1.00
6.25	1.00
8.00	1.00
10.00	1.00
12.50	1.00
16.00	1.00
20.00	1.00
25.00	1.00
31.50	1.00
40.00	1.00
63.00	1.00
80.00	1.00
100.00	1.00
160.00	1.00

200.00	1.00
315.00	1.00
400.00	1.00
500.00	1.00
630.00	1.00
800.00	1.00
1000.00	1.00
1250.00	1.00
1600.00	1.00
2000.00	1.00
2500.00	1.00
3000.00	1.00

2.3. Test Plate set up

The plate was first cleaned with a wipe (VeriGuard 1, IPA Polypropylene Tub Wipe, Micronclean) to remove any glue or other dirt.

Once cleaned, the fixture points for all accelerometers were labelled with the respective serial number for identification purposes, as shown in Figure 1. Tape (3M 1205 Polyimide Tape Amber 25mmx33m, Self-Adhesive Supplies) was applied to the fixture point for the vibration accelerometers, as well as the base of each vibration accelerometer to protect the respective surfaces as shown in Figure 2.

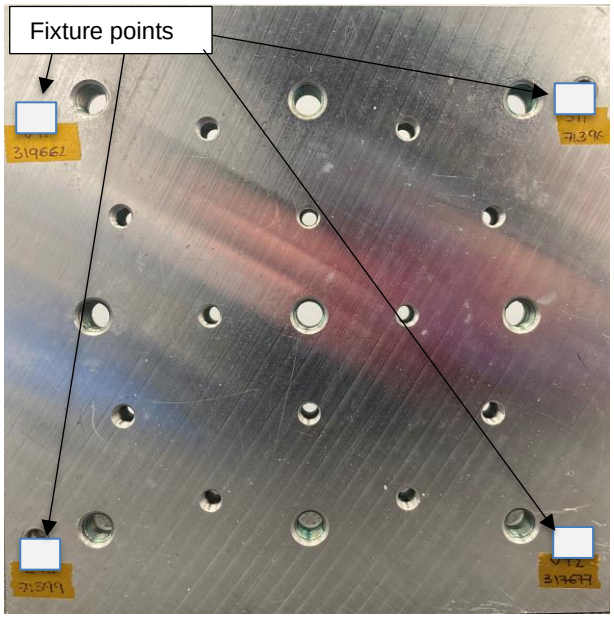

Figure 1: Fixture points and labels identified on the test plate

Figure 2: Example of a vibration accelerometer with applied protective tape

Due to the temperature range, a temperature compatible glue (665-4824, Cyanolube Cyanoacrylate, Electrolube) was required to fix each vibration accelerometer to its fixture point. With a mounting thread of ¼-28 male, the shock accelerometers were screwed into the fixture point prior to being torqued to 2Nm.

As the shock accelerometers come with integrated cables, the cables were coiled, as shown in Figure 3 and secured with tape to prevent entanglement.

Figure 3: Complete test plate set-up

2.4. Thermal Profiling

During the preparation of the test plate, the alternating climate chamber (Model MK 240 – 400V, Dynamic climate chamber, Binder Inc) was preheated for 1 hour at the corresponding test stage/phase temperature.

Once fixed to the plate per the test plate preparation method and the chamber preheat time had elapsed, the accelerometers and test plate were placed into the chamber. Accelerometers were exposed to the thermal profile shown in Figure 4, where progression to the subsequent stage or phase depended on calibration results remaining within the ±5% deviation range.

The order of test stages shown in Figure 4 was decided based on increasing risk of failure and allowed for progressive checking and measuring of accelerometer sensitivity response. All tests were performed with the humidity function switched off to reduce the number of variables in testing. Figure 4 outlines the test stages, which are defined by different combinations of temperature (T) and time (t).

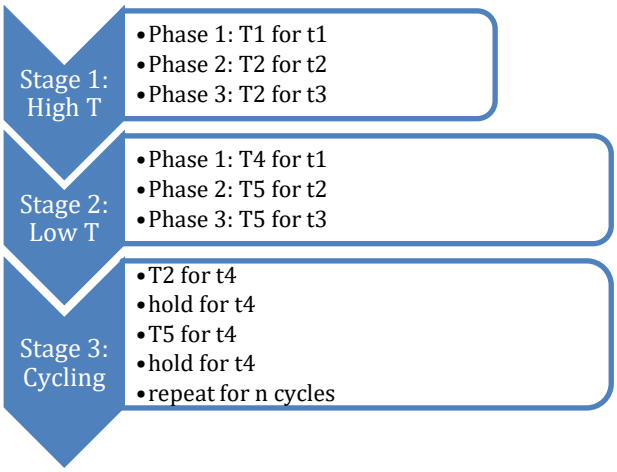

Figure 4: Thermal profile test stage flow diagram

Table 5 details the input parameters for the respective stage 1 and stage 2 phases which operated off a constant state. The time began once the chamber temperature had been restored to the stated temperature following the opening of the door to insert the test plate. Once time had elapsed, the chamber temperature was reduced/ increased to +21˚C (room temperature), where the test plate was left for an additional hour before removing from the chamber.

Table 5: Stage 1 and Stage 2 test temperatures and run times

Stage	Phase	Temperature (˚C)	Run Time (hrs)
1	1	+ 66	2
	2	+ 90	48
	3	+ 90	336
2	1	- 23	2
	2	- 55	48
	3	- 55	336

The inputs for programming stage 3: steady cycling are detailed in Table 6. Once program sections 1 and 2 had elapsed, sections 3 to 6, inclusive, repeated 83 times to produce a cyclic testing profile before completing program sections 7 and 8. The programme in Table 6 cumulates to a test period of 336 hrs, equivalent to stage 1: phase 3 and stage 2: phase 3.

Table 6: Stage 3 test programme inputs

Program Section	Set Point (˚C)	Section Time (mins)
1	21.00	60
2	21.00	60
3	90.00	60
4	90.00	60
5	-55.00	60
6	-55.00	60
7	21.00	60
8	21.00	1/60th

The temperature for each stage/phase was monitored routinely throughout testing to ensure no temperature deviations occurred.

2.5. Sensitivity Analysis

To review the sensitivity shift of the accelerometers, the calibration sensitivities were compiled in a spreadsheet (Microsoft Excel, Microsoft Campus) and subsequently graphed to provide a visual representation.

The ±5% deviation limits were calculated using the nominal accelerometer sensitivity value and allowed for a clear indication of whether the accelerometer sensitivity had deviated past the acceptable limits.

3. RESULTS

Following graphing of sensitivities determined during calibration, the graphs were visually inspected to determine whether the deviation limit had been exceeded. Table 7 consolidates the results of the graphs, where pass indicates that the accelerometer has remained within ±5% deviation of the nominal value for all thermal test stages, and fail indicates that the accelerometer has exceeded the ±5% deviation limits at a stage during the thermal testing profile.

Table 7: Summary of sensitivity graph inspection

Accelerometer	Pass/ Fail?
356A43/ LW317655 (X-axis)	Pass
356A43/ LW317655 (Y-axis)	Pass
356A43/ LW317655 (Z-axis)	Pass
356A43/ LW319662 (X-axis)	Pass
356A43/ LW319662 (Y-axis)	Pass
356A43/ LW319662 (Z-axis)	Pass
356A43/ LW317677 (X-axis)	Pass
356A43/ LW317677 (Y-axis)	Pass
356A43/ LW317677 (Z-axis)	Pass
356A43/ LW317656 (X-axis)	Pass
356A43/ LW317656 (Y-axis)	Pass
356A43/ LW317656 (Z-axis)	Pass
350M88A/ 71397	Pass
350M88A/ 71396	Failed during Stage 3
350M88A/ 71399	Failed during Stage 3
350M88A/ 71398	Failed during Stage 3

Figs. 5-12 show the results of the sensitivity A line was drawn to connect the averages of each set of sensitivities. The top and bottom lines show the ±5% deviation limits between which the accelerometer sensitivity needed to remain within.

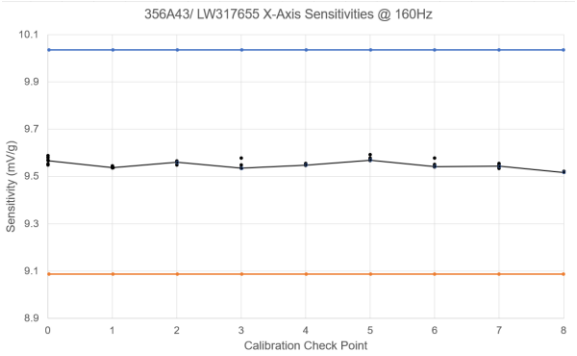

(a)

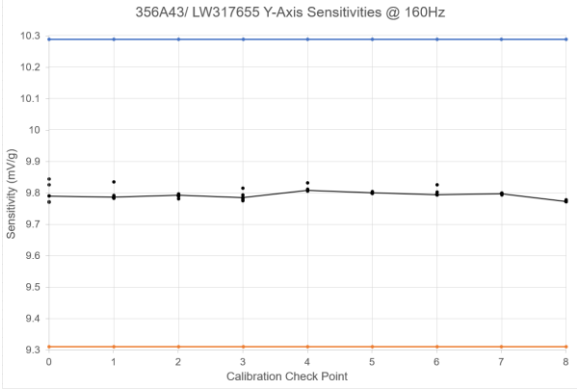

(b)

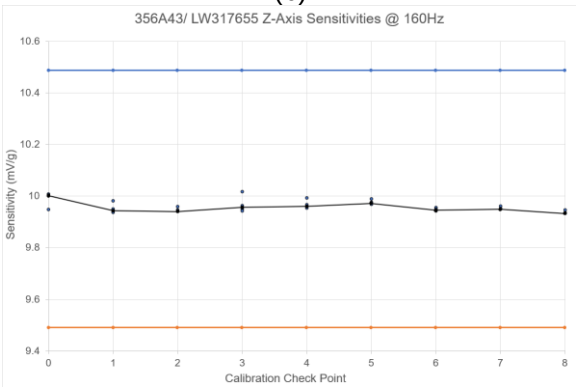

(c)

Figure 5: 356A43/ LW317655 sensitivities @ 160Hz with +/- 5% deviation limits, following test profile, (a) X-axis sensitivities, (b) Y-axis sensitivities, (c) Z-axis sensitivities

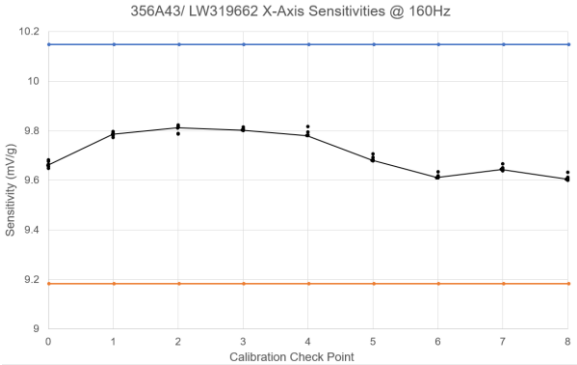

(a)

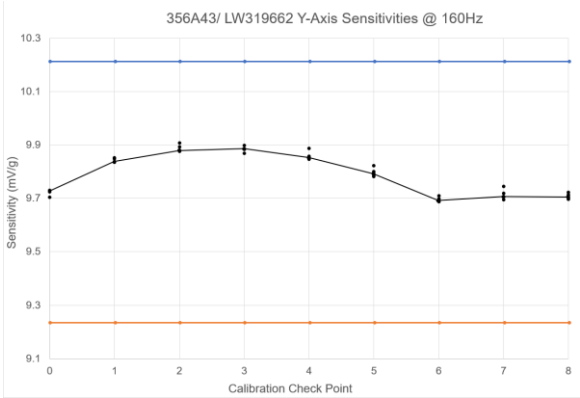

(b)

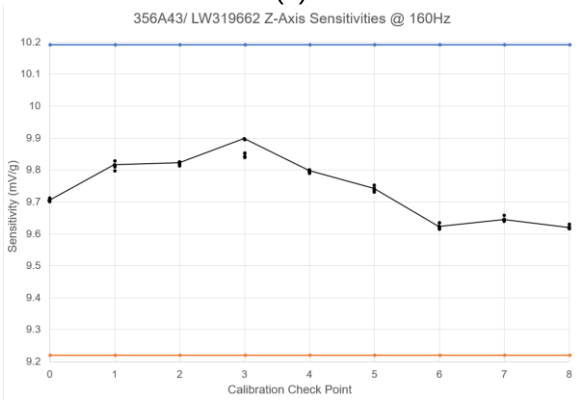

(c)

Figure 6: 356A43/ LW319662 sensitivities @ 160Hz with +/- 5% deviation limit, following thermal profile, (a) X-axis sensitivities, (b) Y-axis sensitivities, (c) Z-axis sensitivities

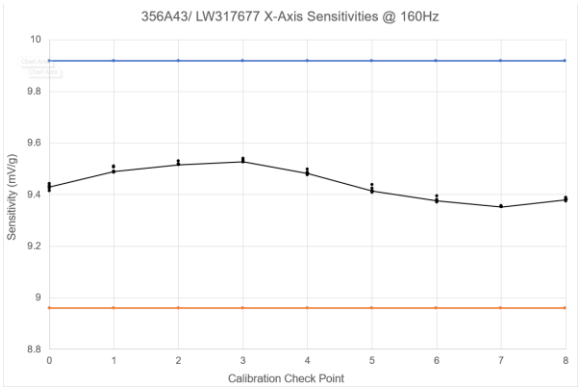

(a)

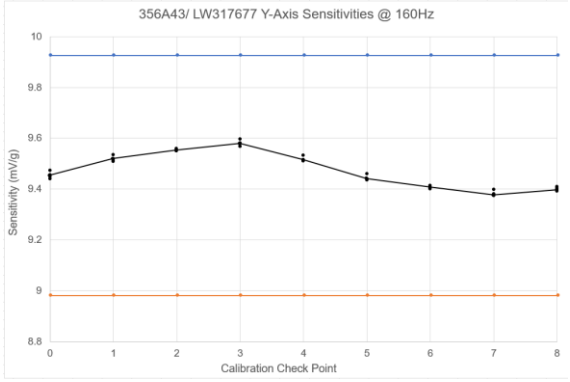

(b)

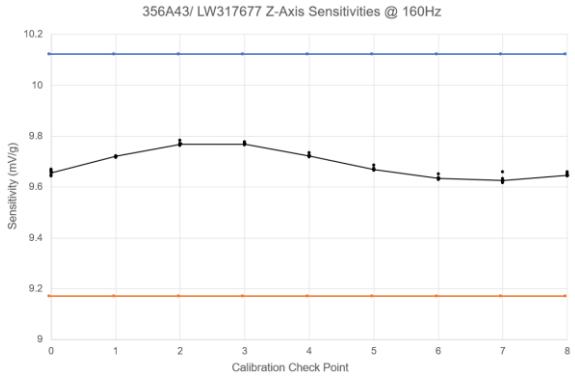

(c)

Figure 7: 356A43/ LW317677 sensitivities @ 160Hz with +/- 5% deviation limit, following thermal profile, (a) X-axis sensitivities, (b) Y-axis sensitivities, (c) Z-axis sensitivities

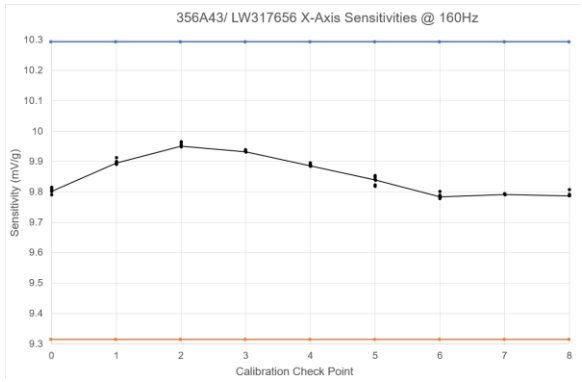

(a)

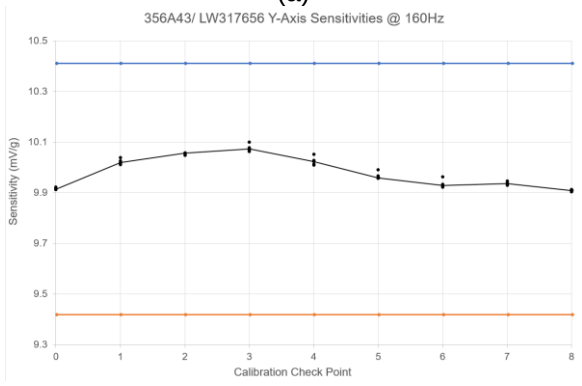

(b)

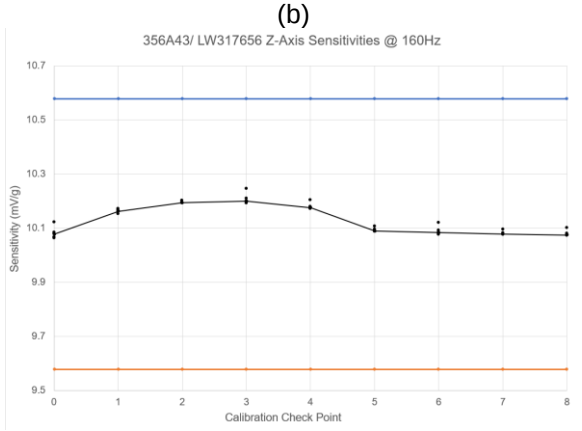

(c)

Figure 8: 356A43/ LW317656 sensitivities @ 160Hz with +/- 5% deviation limit, following thermal profile, (a) X-axis sensitivities, (b) Y-axis sensitivities, (c) Y-axis sensitivities

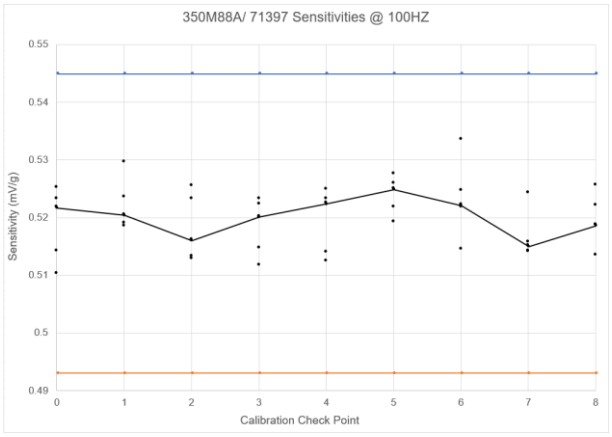

Figure 9: 350M88A/ 71397 sensitivities @ 100Hz with +/- 5% deviation limit following thermal profile

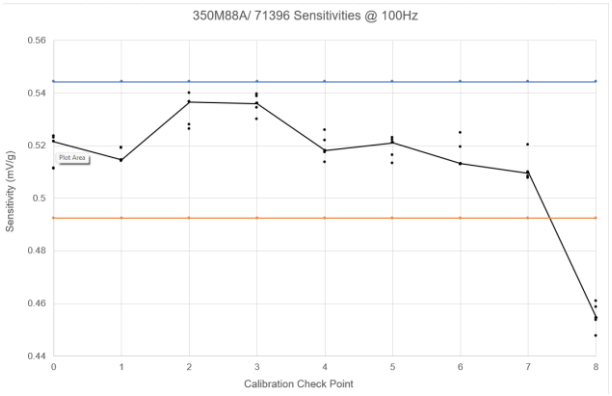

Figure 10: 350M88A/ 71396 sensitivities @ 100Hz with +/- 5% deviation limit following thermal profile

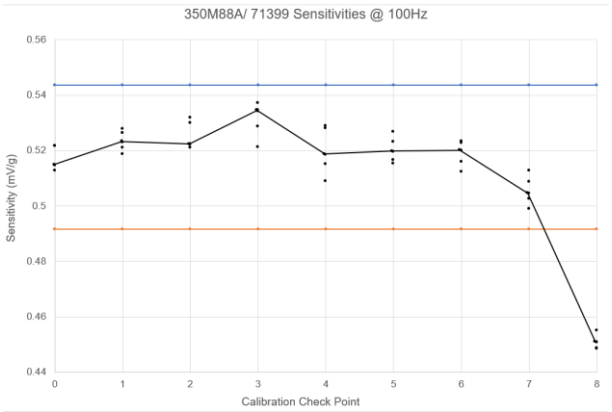

Figure 11: 350M88A/ 71399 sensitivites @ 100Hz with +/- 5% deviation limit following thermal profile

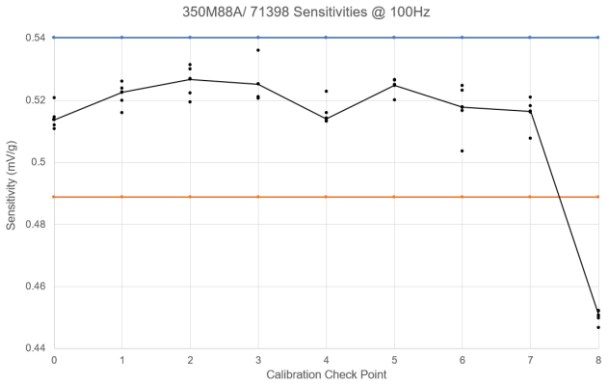

Figure 12: 350M88A/ 71398 sensitivities @ 100Hz with +/- 5% deviation limit following thermal profile.

4. DISCUSSION

The 356A43 vibration accelerometers and singular 350M88A shock accelerometer all passed the thermal testing profile remaining well within the deviation limit, as shown in Tab. 6 and Figs. 5 – 9. Accelerometers 356A43/ LW317655 and 350M88A/ 71397, were expected to pass as they were held as controls and not exposed to the thermal profile. This allowed a level of confidence in the calibration rig to be established and proved a useful reference when analysing the graphs for equivalent models. On this basis, it can be seen for the vibration accelerometers in Figs. 5 – 8 that the curves follow a similar profile. However, the shock accelerometer results in Figs. 10 – 12 display a noticeably different shape compared to the control in Fig. 9. This indicates that the vibration accelerometers (356A43) experienced minimal impact from the thermal profile but that the shock accelerometers (350M88A) were noticeably influenced by the thermal profile.

Regarding the acceptable temperature range, the temperature (operating) of -54 ˚C to +121 ˚C, as detailed in Tab. 2, indicates that the 356A43 vibration accelerometers should be capable of surviving the thermal test profile. Evidence of this can again be seen in Figs. 6 – 8, where the sensitivity remains within ±5%.

Likewise, the temperature (operating) of -23 ˚C to +66 ˚C and temperature (storage) of -40 ˚C to +93 ˚C, detailed in Table 1, indicates that the 350M88A shock accelerometers should not be capable of surviving the thermal testing profile. While Tab. 6 indicates that shock accelerometers 71396, 71399, and 71398 failed overall following the thermal profile. When the sensitivities, calibration check points, and testing stages/ phases are analysed individually, the point of failure can be identified. Across Figs. 10 – 12, the shock accelerometers can be seen to remain within the ±5% deviation limits for calibration check points 1 – 4 that correspond with steady high temperatures. A similar result can be seen across calibration check points 5 – 7 that correspond with the steady low temperatures. However, the shock accelerometers 71396, 71399, and 71398 can be seen to exceed the -5% deviation limit at calibration check point 8, corresponding with the completion of stage 3 testing.

It can therefore be concluded that the steady temperature profiles appear to elicit no mechanical stresses that result in permanent component deformation. However, it can be concluded that steady cycling induces enough mechanical stress to modify the accelerometer's components.

However, while the shock accelerometers have failed regarding the deviation limits set in this test profile, they still elicit an electrical response when run through the calibration rig, meaning that the accelerometer components remain functional to a certain degree.

5. CONCLUSIONS

A sensitivity analysis of accelerometers following thermal cycling was conducted using 356A43 vibration accelerometers and 350M88A shock accelerometers. The existing accelerometer specifications indicated that the shock accelerometers were more likely to experience mechanical stress resulting in failure due to the thermal test profile.

The thermal test profiling comprised of 3 stages: stage 1 – steady high temperature, stage 2 – steady low temperature, and stage 3 – cycling between high and low temperatures. Where stage 1 and stage 2 saw a further decomposition into phases 1 – 3. Phase 1 temperatures were +66 ˚C and – 23 ˚C for stage 1 and stage 2, respectively. In phases 2 and 3, temperatures were +90 ˚C and -55 ˚C for stage 1 and stage 2, respectively.

Accelerometers were calibrated using a vibration calibration rig before the commencement of testing and between progression from one stage/ phase to another. This allowed for constant monitoring of the accelerometers to see each variable's impact.

The resulting sensitivities were compiled in a spreadsheet to create a graphical representation. This enabled visual inspection of sensitivity variation to be conducted and monitor whether the deviation limits had been exceeded.

The methods used and discussed in this study allow for an increased understanding of piezoelectric accelerometers' response to a varied thermal profile test, namely the sensitivity and temperature dependency. This study also highlights the importance of consistent calibration/ sensitivity monitoring of accelerometers, especially when testing near or outside stated temperature limits and remains valuable in providing confidence to vibration, shock, and thermal testing. With regard to further investigation, testing accelerometers with

different technology would be beneficial to further understand how technology may impact response. In addition, further research into modelling the temperature-induced mechanical stresses to predict failure prior to conducting a thermal profile test or non-destructive investigation into the failure cause may also prove beneficial in the development of understanding accelerometers and their behaviour under thermal testing.

6. REFERENCES

1. Dey, A.K. (2022) *What is an Accelerometer? Working, Selection, Application, and Types of Accelerometer,* Available at: *https://whatispiping.com/accelerometer/*
2. Engineering 360 (2022) *Accelerometers Information,* Available at: *https://www.globalspec.com/learnmore/sensors_transducers_detectors/acceleration_vibration_sensing/accelerometers*
3. Arar, S. (2022) *Understanding Piezoelectric Accelerometer Basics,* Available at: *https://www.allaboutcircuits.com/technical-articles/introduction-to-piezoelectric-accelerometers-piezoelectric-sensor-basics*
4. A. Chu, (2012) *Choosing the right type of accelerometers*, Application Notes, Measurement Specialties Inc.
5. Arar, S. (2022) *Accelerometer Specifications: Measurement Range, Sensitivity and Noise Performance,* Available at: *https://www.allaboutcircuits.com/technical-articles/accelerometer-specifications-measurement-range-sensitivity-and-noise-performance/*
6. Mayo, S. (2009) *Understanding Key Accelerometer Specs*, Evaluation Engineering: Electronic Design.
7. Bâzu M, Gălăţeanu L, Ilian VE, Loicq J, Habraken S, Collette J-P. (2007) *Quantitative Accelerated Life Testing of MEMS Accelerometers.* Sensors.; 7(11):2846-2859. https://doi.org/10.3390/s7112846
8. Acar, C. and Shkel, A.M. (2003) '*Experimental evaluation and comparative analysis of commercial variable-capacitance MEMS accelerometers*', *Journal of Micromechanics and Microengineering* , 13, pp. 634-645 [Online]. Available at: *stacks.iop.org/JMM/13/634*